



Influence of Super Cyclone “Amphan” in the Indian Subcontinent amid COVID-19 Pandemic

Shubham Kumar¹ · Preet Lal¹ · Amit Kumar¹

Received: 4 February 2021 / Revised: 18 May 2021 / Accepted: 31 May 2021 / Published online: 12 June 2021
© The Author(s), under exclusive licence to Springer Nature Switzerland AG 2021

Abstract

Tropical cyclone “Amphan” developed as a super cyclone on 19 May 2020 and caused severe impact on the landmass with very high torrential precipitation ($>250 \text{ mm day}^{-1}$), and extremely high wind speed ($>150 \text{ km h}^{-1}$) after landfall on 20 May 2020. The tropical cyclone Amphan largely affected agricultural land (78.2%) and forest, including mangroves (10.8%) in eastern India and Bangladesh. The built-up area over the trajectory of the cyclone and its proximity, including eastern parts of the Kolkata metropolitan area, was considerably affected by the cyclone due to the high population density and poor structural and community planning. Although the regions with close proximities to cyclones’ trajectory (2033 km^2 area under $<2 \text{ km}$ proximity) were affected severely, the presence of mangrove forest in Sundarban substantially reduced the magnitude of the tropical cyclone. A considerable decrease ($\sim 30\%$) in aerosol optical depth (AOD) in April–May 2020 as compared to that in 2019 is considered one of the major causes of the development of the warm pool and cyclogenesis in the Bay of Bengal. The number of COVID-19 cases increased by $\sim 70\%$ in the post-cyclonic period (29 May 2020) compared to that in the pre-cyclonic period (19 May 2020) illustrating the impact of the cyclonic hazard.

Keywords Tropical cyclone · Precipitation · AOD · SST · Mangrove · Bay of Bengal · COVID-19

1 Introduction

The Indian Ocean experienced the devastating impact of super cyclone *Amphan* during 16 May–22 May 2020. Amphan was the first super cyclonic storm in the Bay of Bengal having a very high wind speed ($>200 \text{ km h}^{-1}$) since the 1999 Odisha cyclone [1]. It caused the loss of human lives (72 persons in India and 12 in Bangladesh), high destruction, and damage to public property, which cost ~ 1 lakh crore INR (13.46 billion USD) and the destruction of around 1 million houses as per the initial reports of damage assessment [4].

A tropical cyclone is characterized by intense tropical storms that originate in a warm tropical ocean with low atmospheric pressure, high wind, and heavy precipitations [33]. The intensity of a tropical cyclone is measured based on its

damage on the landmass after landfall [20, 34]. Globally, the Indian subcontinent is considered one of the worst cyclone-affected parts in the Indian ocean region due to the shallow depth and the warm pool phenomenon (sea surface temperature (SST) $\sim > 28 \text{ }^\circ\text{C}$) [14], where the Bay of Bengal (BoB) is more prone to cyclone genesis [2] with an approximate ratio of 4:1 as compared to the Arabian Sea [11]. The Indian Ocean experiences an average of 5–6 cyclonic activities in a year [32], affecting the coastal regions and interior parts with different intensities [10]. The settlements in the coastal areas, primarily major cities, are affected by not only cyclones but also various other natural disasters including sea-level rise [31], storm surge [8], and flood inundation [15, 23, 24].

The occurrence of any natural hazards during the COVID-19 pandemic may have catastrophic and cascading implications [29]. The co-occurrence of hazardous natural (cyclones) and a biological origin (COVID-19) leads to severe crisis situations and challenges the resilience of societies and systems [30]. The COVID-19 pandemic that occurred in December 2019 has created havoc around the globe due to an increase in the number of cases and deaths [22]. The virus outbreak has been spreading through human-to-human transmission [5]. Globally, there were around 148,859,866 confirmed cases

Shubham Kumar and Preet Lal contributed equally and can be treated as first authors.

✉ Amit Kumar
amit.iirs@gmail.com; amit.kumar@uj.ac.in

¹ Department of Geoinformatics, Central University of Jharkhand, Ranchi 835205, India

(with 3,138,755 deaths) reported as of 27 April 2021 (<https://cutt.ly/1bfqU7c>), in which 9.34% and 0.46% of global cases, and 5.90% and 0.32% of global deaths due to COVID-19 were associated with India (<https://www.mohfw.gov.in/>) and Bangladesh (<https://iedcr.gov.bd/>), respectively. Cyclonic impact leads to a transition in season phenomenon and increases the susceptibility of cough, cold, and fever by weakening the immune system of the human body [16], developing similar symptoms to COVID-19 infections [25, 26, 35]. Furthermore, there are high chances of compromising the necessary physical distancing measures during the evacuation process to a safe zone, which increases the risk of COVID-19 infections. Therefore, in the present study, an attempt has been made to examine the movement of tropical cyclone *Amphan* and its impact on the Indian subcontinent, amid the COVID-19 period. Also, the spatio-temporal patterns of SST, aerosol optical depth (AOD), and precipitation during the period of the super cyclone were analyzed to understand the origin and impact of tropical cyclone *Amphan*.

2 Data Used and Methodology

Satellite-based measurements of precipitation, AOD, wind vector analysis, land use/land cover (LULC), SST, and Indian Meteorological Department (IMD) bulletin reports were used to monitor the trajectory of super cyclone *Amphan* and its impact on the region. The forecasted and the final trajectories of the cyclone were mapped using IMD Bulletin reports (Bulletin numbers 01, 09, 17, 25, 30, and 41). Global Precipitation Mission (GPM) (<https://giovanni.gsfc.nasa.gov/giovanni/>) datasets [17] were used to map the variations of daily precipitation along the cyclone track, whereas Oceanic SAF SCATSAT-1 (having 25-km horizontal resolution) during 11 to 21 May 2020 was used to analyze the pattern of wind circulation in the ocean and the movement from the Ocean (Bay of Bengal) to the landmass. Since the origin and movement of cyclones depend on SST, the Group for High-Resolution Sea Surface Temperature (GHRSSST) (<https://podaac.jpl.nasa.gov/GHRSSST>) datasets were evaluated for the period of 01 to 21 May 2020.

MODIS MOD08 D3 v6.1 combined Dark Target and Deep Blue AOD at 0.55 μm for land and ocean of 1-day temporal resolution (<https://giovanni.gsfc.nasa.gov/giovanni/>) [28] datasets were acquired to study the changes in AOD concentration during the period 01 April to 21 May in 2019 as well as analogous in 2020. The percent change in mean AOD during April and May of 2020 has been estimated using mean AOD in the period in 2019 (Eq. 1).

$$\text{Percent Change in AOD} = \left(\frac{\text{Mean AOD 2019} - \text{Mean AOD 2020}}{\text{Mean AOD 2019}} \right) * 100 \quad (1)$$

Proximity analysis of cyclonic path (<2 km, 2–5 km, 5–10 km, and 10–50 km) was performed to deduce the potential impact of cyclones on the LULC in the region. The LULC dataset was acquired from the European Space Agency Climate Change Initiative (ESA-CCI) at 300-m spatial resolution and used to estimate the area of influence of tropical cyclone *Amphan*. The COVID-19 information was acquired using various government reports from India (<https://www.mohfw.gov.in/>) and Bangladesh (<https://iedcr.gov.bd/covid-19/covid-19-general-information>). The pre- and post-cyclonic events of COVID-19 cases were compared at the district and state levels to deduce the implications of natural disasters on the rise in infections.

3 Results and Discussion

3.1 Trajectory of *Amphan* Cyclone

Over its lifetime, the super cyclone *Amphan* had a very long trajectory of ~1820 km, of which 72.96% (1328 km) was observed on the ocean surface and 27.04% (492 km) was observed on the landmass. On 13 May 2020, an anti-clockwise wind pattern (Fig. 1) was observed in the Bay of Bengal at 10°N and 87°E, resulting in the formation of a low-pressure region that created the cyclone *Amphan* (Fig. 2). This low pressure was created as a result of increasing sea temperatures (>32 °C) in the Bay of Bengal, ~1250 km south of West Bengal (WB). This phenomenon lasted until 15 May 2020 and intensified rapidly into a depression during the next subsequent 24 h. On 16 May 2020, it transformed into a depression and shifted northwestward (87°E and 10°N) with low wind speed (>60 km h⁻¹). On 17 May 2020, it converted into a severe cyclonic storm with a moderate wind speed (80–120 km h⁻¹; gusting to 140 km h⁻¹) near 11.4°N and 86.0°E. On 18 May 2020, it intensified into an extremely severe cyclonic storm with a moderately high wind speed (120–150 km h⁻¹; gusting to 180 km h⁻¹). This extremely severe cyclone moved northwards during the subsequent 24 h and transformed into a super cyclone on 19 May 2020 with a very high wind speed (200–250 km h⁻¹; gusting to 250 km h⁻¹) near around 670 km south–southwest to the coast of WB. The super cyclone lost its energy on 20 May 2020 and weakened into an extremely severe cyclonic storm while moving northwards near the coast of WB. The landfall of the *Amphan* cyclone occurred on 20 May 2020 afternoon (~1430 h IST) at the coast of WB, India (at Bakkhali in Sundarban delta) with a high wind speed (~150–160 km h⁻¹; gusting to 180 km h⁻¹). It passed through WB state on 20 May 2020 evening hours (1800 h IST) with high wind speed (155–165 km h⁻¹) and reached Bangladesh with

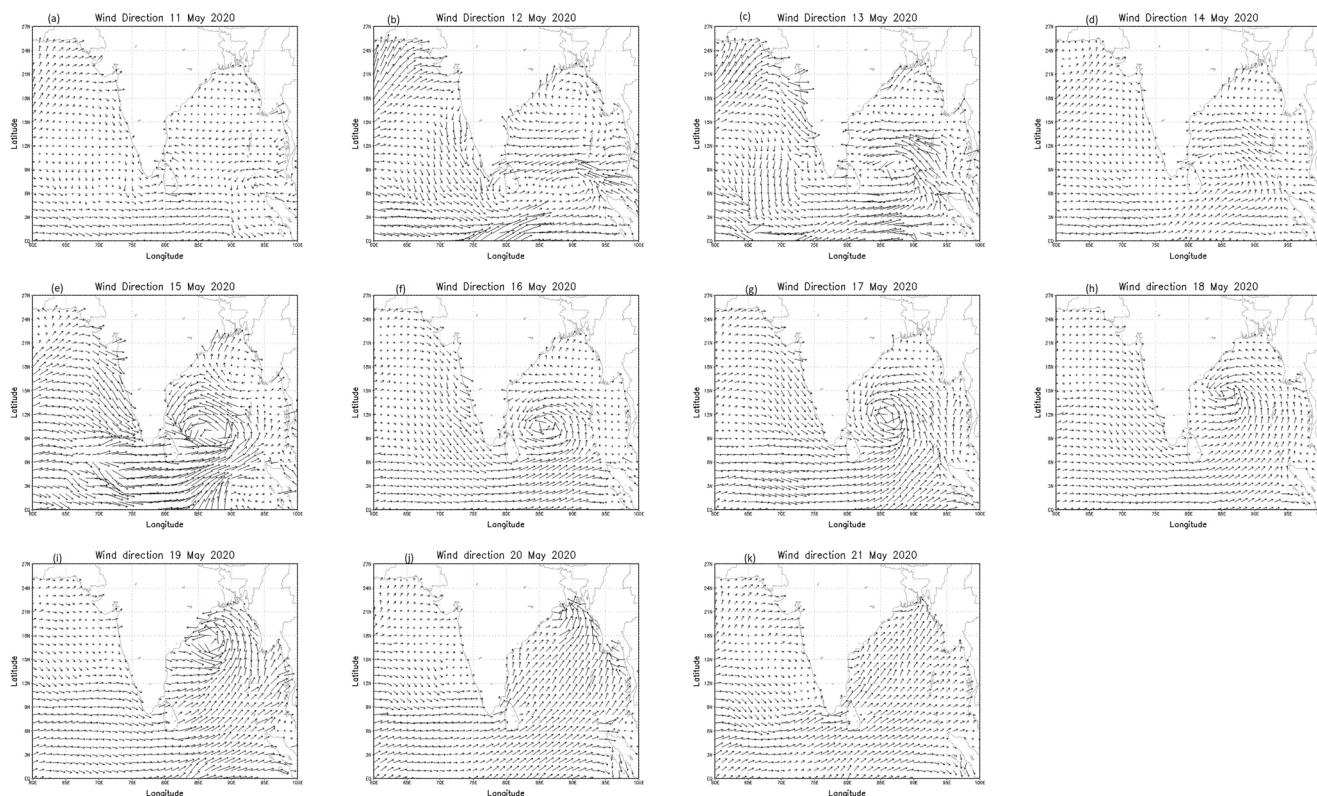


Fig. 1 Wind movement across the sea surface during 11–21 May 2020 based on SAF SCATSAT oceanic satellite data

decreasing intensity to severe cyclonic storm. On 21 May 2020, it further transformed to a cyclonic storm by losing its strength and later converted into a low pressure on 21 May 2020 during evening hours (at ~ 1800 h IST) with a very low wind speed (<40 km h $^{-1}$) and eventually lost its existence near the Indo-Bangladesh border (26.2°N , 90.7°E). The cyclone caused widespread destruction in districts of India (South 24 Pargana, North 24 Pargana, Hooghly, Howrah, and Purba Medinipur of West Bengal State) and Bangladesh (Rajshahi, Nator, Pabna, Khustia, Meherpur, Chuadanga, Jinaldaha, Magura, Jessore, Meherpur, and Satkhira) along its trajectory and vicinity. The forecasted trajectory of tropical cyclone Amphan (by IMD) was similar to the actual trajectory despite a high deviation from the forecasted trajectory in the ocean in the initial days of forecasting (Fig. 2).

3.2 AOD and SST

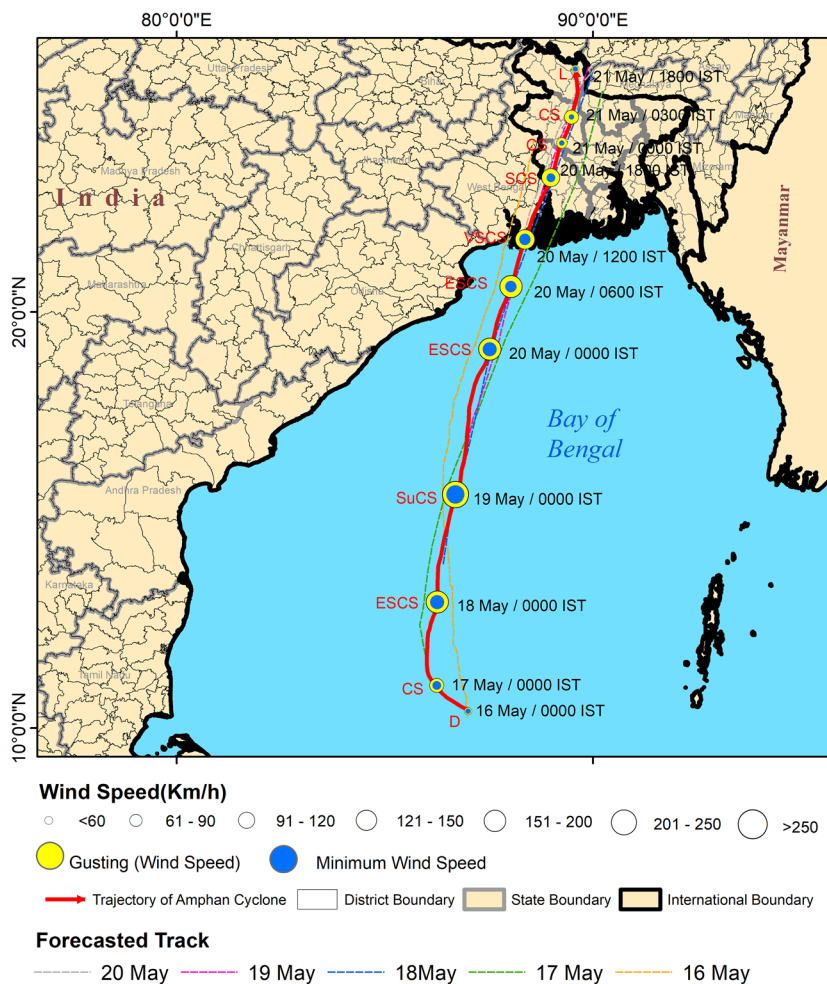
The low concentration of aerosols in the atmosphere has a warming effect, which increases the frequency of formation of cyclones of varying intensities [36]. The COVID-19 pandemic induced lockdown in India (phase 1: 25 March 2020 to 31 May 2020) and Bangladesh (phase 1: from 22 March 2020 to 30 May 2020) resulting in a rapid decline in concentration of AOD in the Indian subcontinent [21] and in the Bay of

Bengal. An average $\sim 30\%$ decrease in AOD was observed in a large (primarily in the southeastern) part of BoB from 01 April to 21 May 2020 compared to its analogous period in 2019 (Fig. 3aa). This may result in the conspicuous warming of ocean surfaces as observed through rising SST in Bay of Bengal effectively on 03 May 2020 (primarily in its southeastern parts with SST $>31^{\circ}\text{C}$). The extent of high SST ($>32^{\circ}\text{C}$) was observed from 10 May to 13 May 2020, leading to the formation of depression on 16 May 2020, and its intensification as an extremely severe cyclone on 19 May 2020 (Fig. 3ab). In contrast, the northern parts of the Indian Ocean and the Arabian Sea observed a low to moderate increase in the AOD ($<-10\%$) in April–May 2020 compared to its analogous period in 2019 (April–May). Previous studies (e.g., [3, 12]) reported that increases in aerosol loads in the ocean surfaces tend to reduce sea surface radiation while decreases in AOD tend to lead to the considerable rise in SST [6, 9, 13, 27].

3.3 Precipitation Analysis

The southern parts of Bay of Bengal recorded relatively high to extremely high precipitation (>250 mm day $^{-1}$) due to the formation of low pressure since 13 May 2020 (Fig. 4). The

Fig. 2 Actual and forecasted trajectories of the Amphan cyclone during 16–21 May 2020 (with time details)



extremely high precipitation continued to shift northward (towards the eastern Indian region) during the process of cyclonic movement in the ocean (16–19 May 2020). On 19 May 2020, the coverage of extremely high precipitation was

maximum with major coverage in northern Bay of Bengal. But it significantly affected the eastern coasts and eastern India (Odisha, WB, Andhra Pradesh, Jharkhand, and Bihar) and southern Bangladesh with very high torrential

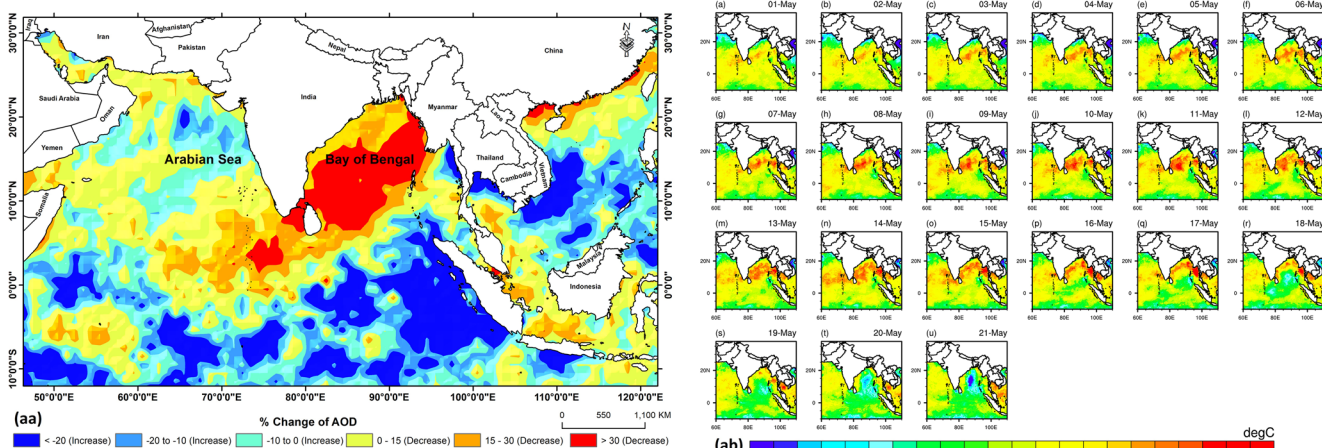


Fig. 3 (aa) MODIS-based percentage change in AOD in 2020 (mean of 01 April to 21 May) with respect to the analogous period in 2019 over North Indian Ocean, and (ab) variation of SST in the North Indian Ocean during 01–21 May 2020

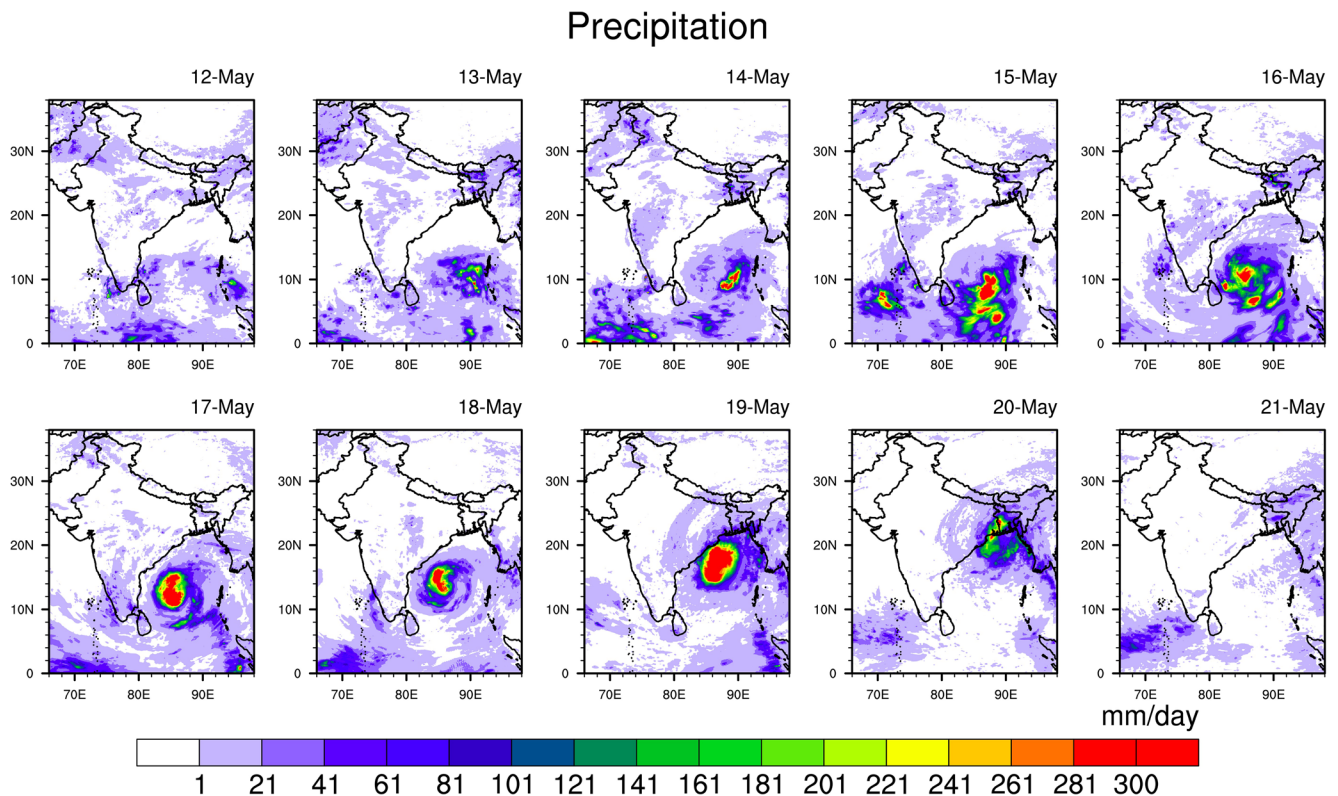


Fig. 4 Precipitation patterns in Bay of Bengal during the Amphan cyclonic period (12–21 May 2020)

precipitation ($140\text{--}250\text{ mm day}^{-1}$). With the landfall on 20 May 2020, the cyclone caused very high precipitation in eastern India and in western Bangladesh. On 21 May 2020, the cyclone-induced precipitation dramatically reduced to a low to very low level by losing its intensity.

3.4 Impact of Amphan Cyclone

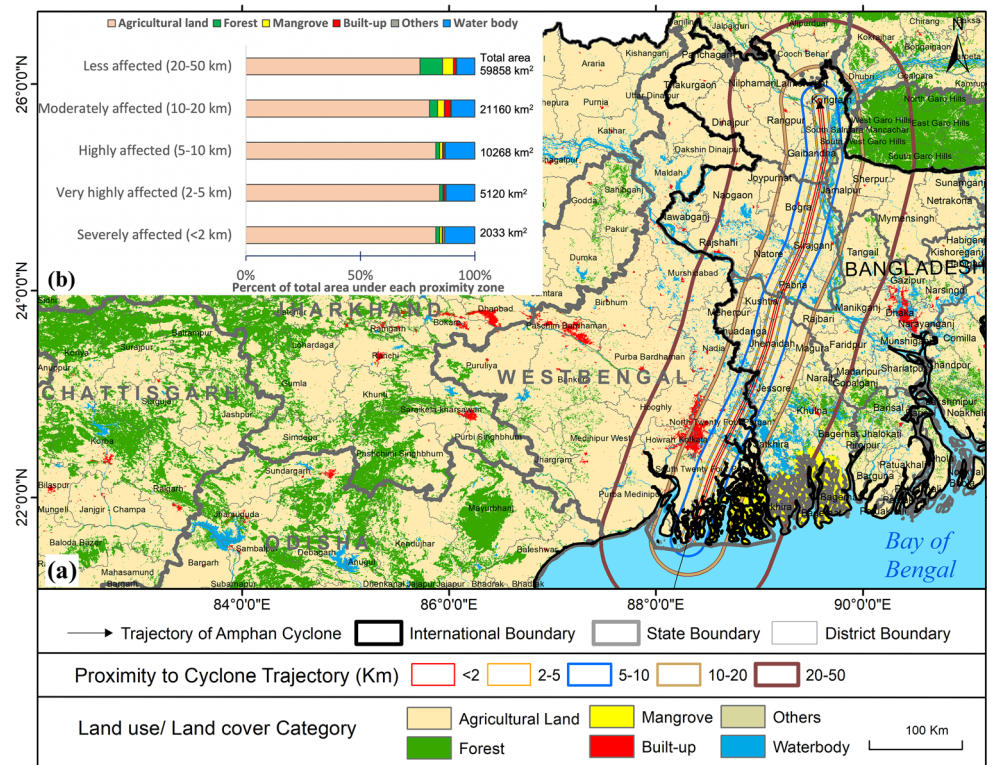
The Amphan cyclone largely affected the agricultural land (78.2%), followed by inland water body (9.3%), forest (7.0%), mangrove (3.8%), built-up (1.4%), and others (0.3%) in eastern India, and Bangladesh after its landfall with different intensities (Fig. 5). The severe impact of the cyclone within the closest proximity to the cyclones' trajectory ($<2\text{ km}$) was significantly evident on agricultural land (1668.79 km^2), followed by forest cover (35.2 km^2), mangrove (20.7 km^2), and others (water body and barren land; 8.55 km^2). Although the total area under the severely affected zone ($<2\text{ km}$ of cyclone trajectory) was smaller (2033 km^2) compared to the highly affected ($5\text{--}10\text{ km}$; $10,268\text{ km}^2$) and moderately affected ($10\text{--}20\text{ km}$; $21,160\text{ km}^2$) areas, the damage was more devastating in the neighboring proximity zones ($<2\text{ km}$) to the cyclone trajectory. Nevertheless, the proportion of built-up area was very significant (1.4% of the total area under $>50\text{ km}^2$ proximity of cyclone), and experienced the catastrophic impact due to high concentration of population and variations in built-up structures. One of the most populated cities of eastern India, the Kolkata metropolitan region that fell under

the moderately affected zone ($10\text{--}20\text{ km}$) observed large destruction in the southern and eastern urban and suburban regions. The cyclone passed through the Sundarbans and affected a large proportion ($\sim 3703.77\text{ km}^2$) of the world's largest mangrove system. Although Amphan cyclone-affected $\sim 36.7\text{ km}^2$ of mangrove forest with severe to very high levels of impact, the mangroves contributed to reducing the cyclonic wind speed and breaking the waves generated by the storm surges during the landfall due to the strong structure of the plants.

3.5 Consequences of the Passage of Amphan Cyclone in the COVID-19 Pandemic Scenario

The world has been facing the severity of the COVID-19 pandemic since late February 2020, which engulfed major parts of the world. In India, the state government of Odisha and WB released directives for evacuation in affected districts in order to maintain social distance amid COVID-19. Only 33% capacity of the shelters in Odisha while 40% capacity of the shelters (500,000 shelters for 200,000 population) in WB were used for evacuees to maintain the physical distance among them [7]. Apart from permanent shelters, governments have also used temporary shelters in schools, community centers, and temporary medical centers (<https://www.bbc.com/news/world-asia-india-52718826>). Bangladesh also managed to evacuate its citizens by maintaining a physical distance and ensuring 12,000 temporary shelters with a capacity of 5.19

Fig. 5 (a) Impact of Amphan cyclone on ESA CCI-based land use/land cover within different proximities to cyclone trajectory, and (b) its area statistic



million population for 2.2 million evacuees with proper supplies of food and emergencies [18]. The timely evacuation of ~4.2 million people living along the coast and in the proximity of cyclone trajectory in India and Bangladesh [19], and the presence of the world’s largest contiguous Sundarbans mangrove, contributed in decreasing the intensity of the Amphan cyclone after landfall (<https://bit.ly/3dn3WH0>). Despite the efficient arrangements to deal with the Amphan cyclone, it caused a death toll of 84 persons and very costly damage to properties due to strong cyclonic winds. A significant rise in confirmed cases of COVID-19 infections in Odisha (by

76.2%; rise from 978 to 1723 cases), Bangladesh (by 70.6%; rise 25,121 to 42,844 cases), and West Bengal (62.5%; rise from 2961 to 4813 cases), with the major increase in Howrah (60.4%) followed by South 24 Pargana (43.3%), North 24 Pargana (38.60%), and Hooghly (37.80%), was observed in the post-cyclonic period (29 May 2020) compared to the pre-cyclonic period (19 May 2020; Table 1). The cyclonic hazard accelerated the COVID-19 infections in the region (<https://www.mohfw.gov.in/>; <https://corona.gov.bd/>), and also affected the preparedness, mitigation, and response mechanisms to cyclonic hazard. There were high chances of compromising

Table 1 Details of COVID-19 cases in the affected states and major affected districts during pre-cyclone and post-cyclone (May 2020)

States/districts	Pre-cyclone COVID-19 cases (until 19 May 2020)	Post-cyclone COVID-19 cases (until 29 May 2020)	% change
Odisha	978	1723	76.2%
West Bengal (WB)	2961	4813	62.5%
Bangladesh	25,121	42,844	70.6%
South 24 Pargana (WB)	102	180	43.3%
North 24 Pargana (WB)	396	645	38.60%
Hooghly (WB)	153	246	37.80%
Howrah (WB)	625	940	33.51%
Purba Medinipur (WB)	51	83	62.74%

COVID-19-related preventive measures during the evacuation process (preparedness) and thus likely to increase the COVID-19 infections. Such overlapping of concurrent hazardous events (i.e., Amphan cyclone and COVID-19) in time and space increased the severity of the crisis, and also challenged the resilience of systems and societies [30].

The present study is based on satellite-based observations for monitoring and assessment of the cyclone hazard and its impact on regional land use/land cover. A regional climate model is required to quantify the changes observed in the aerosol concentration and to deduce its impact on sea surface temperature and radiations.

4 Conclusion

A considerable rise in SST ($>32\text{ }^{\circ}\text{C}$) in the southern Bay of Bengal contributed to the formation of super cyclone Amphan, which moved northwards and affected a large proportion of area in eastern India and Bangladesh after landfalls (20 May 2020) with very high torrential precipitation ($140\text{--}250\text{ mm day}^{-1}$), and extremely high wind speed ($>150\text{ km h}^{-1}$). The Amphan cyclone largely affected the agricultural land (78.2%) and forest (10.8%) in eastern India and Bangladesh. The 1.4% (36.5 km^2) built-up area was considerably affected by the Amphan cyclone due to the high concentration of population and variations in built-up structures. A considerable decrease ($\sim 30\%$) in AOD during April–May 2020 compared to that in 2019 was observed due to COVID-19-induced lockdown, which resulted in a conspicuous rise in SST and formation of Amphan cyclone. This result is consistent with previous studies that concluded that changes in AOD influence SST [6, 9, 13, 27]. The accurate forecasting of the trajectory of the Amphan cyclone contributed to effective preparedness, and response to the cyclonic hazard in the region in the COVID-19 pandemic-affected scenario, leading to moderate death tolls.

Acknowledgements The authors sincerely thank the anonymous reviewers and the Editor of the Journal for reviewing the manuscript and providing critical comments to improve the quality of the paper. The authors acknowledge the Indian Meteorological Department (IMD) for producing the Bulletin reports; Giovanni (NASA) for archiving NRT-GPM and AOD datasets; PODAAC for archiving GHRSSST datasets; and ESA-CCI for archiving LULC datasets.

Code Availability GEE Code can be made available through user request.

Data Availability Data can be made available through user request.

Declarations

Conflict of Interest The authors declare no competing interests.

References

- Ahmed R, Mohapatra M, Dwivedi S, Giri RK (2021) Characteristics features of super cyclone ‘AMPHAN’- observed through satellite images. *Trop Cyclone Res Rev*. <https://doi.org/10.1016/j.tcr.2021.03.003>
- Alam MM, Hossain MA, Shafee S (2003) Frequency of Bay of Bengal cyclonic storms and depressions crossing different coastal zones. *Int J Climatol* 23:1119–1125. <https://doi.org/10.1002/joc.927>
- Allen RJ, Norris JR, Wild M (2013) Evaluation of multidecadal variability in CMIP5 surface solar radiation and inferred underestimation of aerosol direct effects over Europe, China, Japan, and India. *J Geophys Res Atmospheres* 118:6311–6336. <https://doi.org/10.1002/jgrd.50426>
- Bag S (2020) Cyclone devastates Kolkata and leaves scores dead. *BBC News*
- Bai Y, Yao L, Wei T, Tian F, Jin D-Y, Chen L, Wang M (2020) Presumed asymptomatic carrier transmission of COVID-19. *Jama* 323:1406–1407
- Bogdanoff AS, Westphal DL, Campbell JR, Cummings JA, Hyer EJ, Reid JS, Clayson CA (2015) Sensitivity of infrared sea surface temperature retrievals to the vertical distribution of airborne dust aerosol. *Remote Sens Environ* 159:1–13. <https://doi.org/10.1016/j.rse.2014.12.002>
- Brackett R (2020) India, Bangladesh tell millions to evacuate as tropical cyclone Amphan approaches. *Weather Channel*
- Chen J, Wang Z, Tam C-Y, Lau N-C, Lau D-SD, Mok H-Y (2020) Impacts of climate change on tropical cyclones and induced storm surges in the Pearl River Delta region using pseudo-global-warming method. *Sci Rep* 10:1965. <https://doi.org/10.1038/s41598-020-58824-8>
- Cheng Y, Lohmann U, Zhang J, Luo Y, Liu Z, Lesins G (2005) Contribution of changes in sea surface temperature and aerosol loading to the decreasing precipitation trend in southern China. *J Clim* 18:1381–1390. <https://doi.org/10.1175/JCLI3341.1>
- De Dominicis M, Wolf J, Jevrejeva S, Zheng P, Hu Z (2020) Future interactions between sea-level rise, tides and storm surges in the world’s largest urban area. *Geophys Res Lett* e2020GL087002
- Dube S, Rao A, Sinha P, Murty T, Bahulayan N (1997) Storm surge in the Bay of Bengal and Arabian Sea the problem and its prediction. *Mausam* 48:283–304
- Dwyer JG, Norris JR, Ruckstuhl C (2010) Do climate models reproduce observed solar dimming and brightening over China and Japan? *J Geophys Res Atmospheres* 115. <https://doi.org/10.1029/2009JD012945>
- Folini D, Wild M (2015) The effect of aerosols and sea surface temperature on China’s climate in the late twentieth century from ensembles of global climate simulations. *J Geophys Res Atmospheres* 120:2261–2279. <https://doi.org/10.1002/2014JD022851>
- Gadgil S, Joseph PV, Joshi NV (1984) Ocean–atmosphere coupling over monsoon regions. *Nature* 312:141–143. <https://doi.org/10.1038/312141a0>
- Gupta K (2020) Challenges in developing urban flood resilience in India. *Philos Trans R Soc A* 378:20190211
- Hassi J, Rytkönen M, Kotaniemi J, Rintamäki H (2005) Impacts of cold climate on human heat balance, performance and health in circumpolar areas. *Int J Circumpolar Health* 64:459–467. <https://doi.org/10.3402/ijch.v64i5.18027>
- Huffman G, Bolvin D, Braithwaite D, Hsu K, Joyce R, Xie P (2014) Integrated multi-satellite retrievals for GPM (IMERG), version 4.4. NASA’s Precipitation Processing Center
- Islam MT, Charlesworth M, Aurangojeb M, Hemstock S, Sikder SK, Hassan MS, Dev PK, Hossain MZ (2021) Revisiting disaster

- preparedness in coastal communities since 1970s in Bangladesh with an emphasis on the case of tropical cyclone Amphan in May 2020. *Int J Disaster Risk Reduct* 58:102175. <https://doi.org/10.1016/j.ijdrr.2021.102175>
19. JNA-Bangladesh (2020) Cyclone Amphan - Joint Needs Assessment (JNA). Needs Assessment Working Group (NAWG)
 20. Kumar S, Lal P, Kumar A (2020) Turbulence of tropical cyclone ‘Fani’ in the Bay of Bengal and Indian subcontinent. *Nat Hazards* 103:1613–1622. <https://doi.org/10.1007/s11069-020-04033-5>
 21. Lal P, Kumar A, Bharti S, Saikia P, Adhikari D, Khan ML (2021) Lockdown to contain the COVID-19 pandemic: an opportunity to create a less polluted environment in India. *Aerosol Air Qual Res* 21:200229. <https://doi.org/10.4209/aaqr.2020.05.0229>
 22. Lal P, Kumar A, Kumar S, Kumari S, Saikia P, Dayanandan A, Adhikari D, Khan ML (2020a) The dark cloud with a silver lining: assessing the impact of the SARS COVID-19 pandemic on the global environment. *Sci Total Environ* 732:139297. <https://doi.org/10.1016/j.scitotenv.2020.139297>
 23. Lal P, Prakash A, Kumar A (2020b) Google Earth Engine for concurrent flood monitoring in the lower basin of Indo-Gangetic-Brahmaputra plains. *Nat Hazards* 104:1947–1952. <https://doi.org/10.1007/s11069-020-04233-z>
 24. Lal P, Prakash A, Kumar A, Srivastava PK, Saikia P, Pandey AC, Srivastava P, Khan ML (2020c) Evaluating the 2018 extreme flood hazard events in Kerala, India. *Remote Sens Lett* 11:436–445. <https://doi.org/10.1080/2150704X.2020.1730468>
 25. Menni C, Valdes AM, Freidin MB, Sudre CH, Nguyen LH, Drew DA, Ganesh S, Varsavsky T, Cardoso MJ, El-Sayed Moustafa JS, Visconti A, Hysi P, Bowyer RCE, Mangino M, Falchi M, Wolf J, Ourselin S, Chan AT, Steves CJ, Spector TD (2020) Real-time tracking of self-reported symptoms to predict potential COVID-19. *Nat Med* 26:1037–1040. <https://doi.org/10.1038/s41591-020-0916-2>
 26. Parra A, Juanes A, Losada CP, Álvarez-Sesmero S, Santana VD, Martí I, Urricelqui J, Rentero D (2020) Psychotic symptoms in COVID-19 patients. A retrospective descriptive study. *Psychiatry Res* 291:113254. <https://doi.org/10.1016/j.psychres.2020.113254>
 27. Patil N, Venkataraman C, Muduchuru K, Ghosh S, Mondal A (2019) Disentangling sea-surface temperature and anthropogenic aerosol influences on recent trends in South Asian monsoon rainfall. *Clim Dyn* 52:2287–2302. <https://doi.org/10.1007/s00382-018-4251-y>
 28. Platnick S, Hubanks P, Meyer K, King M (2014) MYD08_M3 MODIS/Aqua Aerosol Cloud Water Vapor Ozone Monthly L3 Global 1Deg CMG. https://doi.org/10.5067/MODIS/MYD08_M3.006
 29. Quigley MC, Saunders W, Massey C, Van Dissen R, Villamor P, Jack H, Litchfield N (2020a) The utility of earth science information in post-earthquake land-use decision-making: the 2010–2011 Canterbury earthquake sequence in Aotearoa New Zealand. *Nat Hazards Earth Syst Sci* 20:3361–3385. <https://doi.org/10.5194/nhess-20-3361-2020>
 30. Quigley MC, Attanayake J, King A, Prideaux F (2020b) A multi-hazards earth science perspective on the COVID-19 pandemic: the potential for concurrent and cascading crises. *Environ Syst Decis* 40:199–215. <https://doi.org/10.1007/s10669-020-09772-1>
 31. Siegel FR (2020) An example of coastal cities hazard exposure and economics. In: Siegel FR (ed) Adaptations of coastal cities to global warming, sea level rise, climate change and endemic hazards. Springer International Publishing, Cham, pp 63–69
 32. Singh O, Khan TMA, Rahman MS (2001) Has the frequency of intense tropical cyclones increased in the North Indian Ocean? *Curr Sci* 575–580
 33. Wong KY, Yip CL, Li PW (2008) Automatic tropical cyclone eye fix using genetic algorithm. *Expert Syst Appl* 34:643–656
 34. Yamaguchi M, Chan JCL, Moon I-J, Yoshida K, Mizuta R (2020) Global warming changes tropical cyclone translation speed. *Nat Commun* 11:47. <https://doi.org/10.1038/s41467-019-13902-y>
 35. Yuki K, Fujiogi M, Koutsogiannaki S (2020) COVID-19 pathophysiology: a review. *Clin Immunol* 215:108427. <https://doi.org/10.1016/j.clim.2020.108427>
 36. Zhao L, Wang S-YS, Becker E, Yoon J-H, Mukherjee A (2020) Cyclone Fani: the tug-of-war between regional warming and anthropogenic aerosol effects. *Environ Res Lett* 15:094020. <https://doi.org/10.1088/1748-9326/ab91e7>

Publisher's Note Springer Nature remains neutral with regard to jurisdictional claims in published maps and institutional affiliations.